back

Bounds on the superconducting transition temperature

Mohit Randeria

https://doi.org/10.1142/S0217984924300047 | **Cited by:** 0 **(Source: Crossref)**

Next >

Abstract

I summarize recent progress on obtaining rigorous upper bounds on superconducting transition temperature T_c in two dimensions independent of pairing mechanism or interaction strength. These results are derived by finding a general upper bound for the superfluid stiffness for a multi-band system with arbitrary interactions, with the only assumption that the external vector potential couples to the kinetic energy and not to the interactions. This bound is then combined with the universal relation between the superfluid stiffness and the Berezinskii–Kosterlitz–Thouless T_c in 2D. For parabolic dispersion, one obtains the simple result that $k_B T_c \leq E_F / 8$, which has been tested in recent experiments. More generally, the bounds are expressed in terms of the optical spectral weight and lead to stringent constraints for the T_c of low-density, strongly correlated superconductors. Results for T_c bounds for models of flat-band superconductors, where the kinetic energy vanishes and the vector potential must couple to interactions, are briefly summarized. Upper bounds on T_c in 3D remains an open problem, and I describe how questions of universality underlie the challenges in 3D.

Keywords: Superconductivity ▪ strongly correlated electrons ▪ flat bands ▪ BCS-BEC crossover

1. Introduction

transition temperature T_c, where we have obtained sharp results in two dimensions (2D), with connections to many interesting experiments.[4,5,6]

This is a contribution to a volume on 50 years of the renormalization group (RG), dedicated to the memory of Michael E. Fisher, and it may seem ironic that I have chosen to focus on that most *non*-universal of quantities, the transition temperature T_c, even though it is a quantity of great general interest for superconductivity! There are, however, many aspects of the analysis presented in the following that I am sure Michael would have approved of. First, these are rigorous[a] bounds on T_c, which do not make any mean-field or other uncontrolled approximations. Second, our derivation of Tc bounds in 2D makes use in a crucial way universal results from the RG analysis of the Berezinskii–Kosterlitz–Thouless (BKT) transition. Finally, universality and quantum critical phenomena play an important role in understanding the unresolved challenges that arise in attempting to prove similar bounds in 3D.

Let me note at the outset that there is no upper bound on the superconducting T_c measured in Kelvin. Superconductivity at 250 K has been established in high-pressure experiments on hydrogen-based materials like LaH.[7] It is widely believed that superfluidity of paired neutrons occurs at $T_c \simeq 10^9 K$ in neutron stars, but then all energy scales here are huge compared to terrestrial quantum materials, e.g. the Fermi energy $E_F \simeq 10 - 100\,\mathrm{MeV}$.

An insightful way to organize data on diverse superconductors is the Uemura plot[8] of $\log T_c$ versus $\log E_F$ in Fig. 1. There is considerable ambiguity in defining "the Fermi energy" E_F in strongly correlated and multi-band materials, nevertheless, the data strongly suggest that all known superconductors have a T_c that scales at most like a constant times E_F. The systems that come closest to a presumed bound are magic-angle twisted bilayer graphene,[5] monolayer FeSe/STO,[6] and ultracold Fermi gases ^{40}K and ^{6}Li in the BCS–BEC crossover,[9] which have little in common except that they are all strongly correlated superconductors or paired superfluids.

back

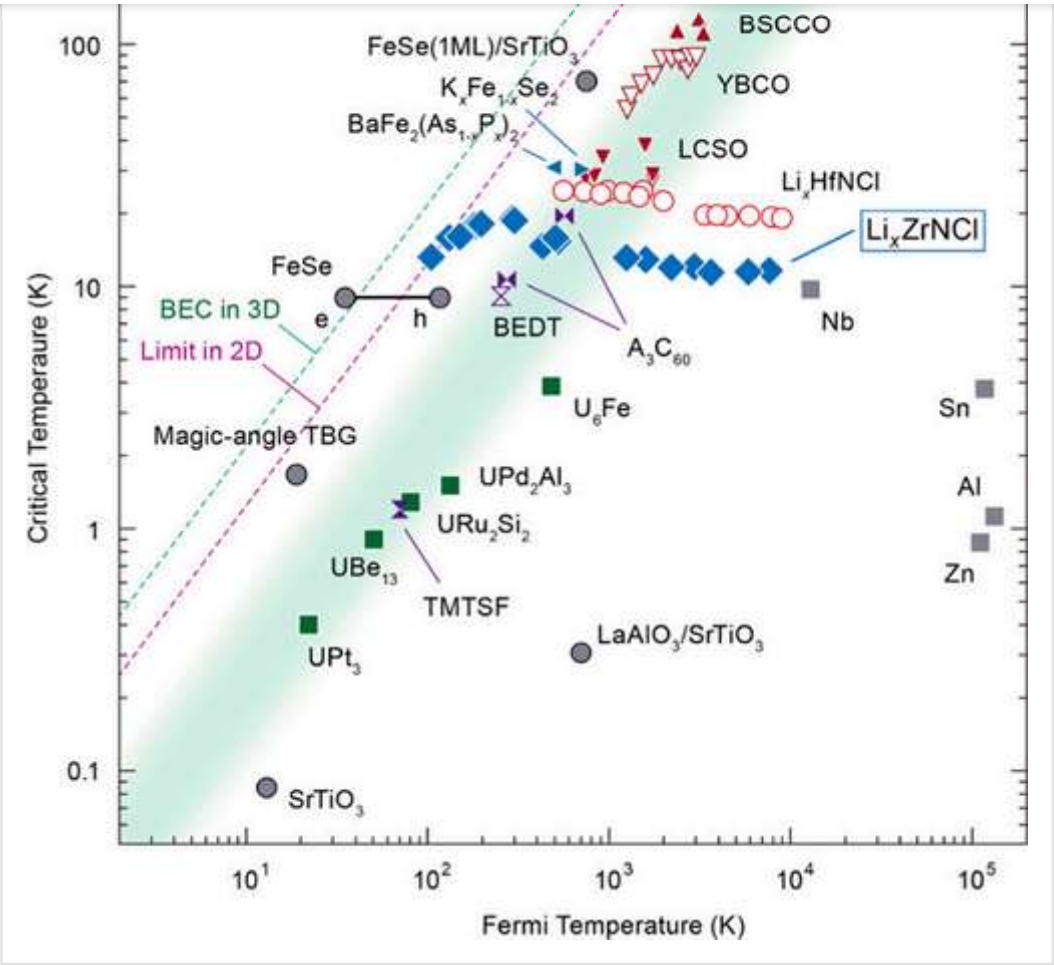

Fig. 1. (Color online) Uemura plot of critical temperature T_c versus Fermi temperature $T_F = E_F \,/\, k_B$ for various superconductors; see text for more details. There are many conventional BCS superconductors in the lower right region (below the green shaded band) that are not shown, however there are no materials in the upper left region. The "limit in 2D" line $T_c = T_F \,/\, 8$ is the 2D bound derived in Ref. **1** for a parabolic dispersion. This bound, together with the Li_xZrNCl data (filled diamonds) from Ref. **4**, are discussed in Sec. 6. T_c bounds for arbitrary dispersion and multi-band superconductors are described in later sections. We discuss in Sec. 11 why the 3D BEC temperature $T_c = 0.218\, T_F$ is *not* a bound on the superconducting T_c in three-dimensional systems. This figure from Ref. **4** is reprinted with permission from AAAS.

These data motivated us to see if one could prove such a bound. The rest of this paper summarizes the progress we have made in 2D, recent experiments on Li:ZrNCl[4] that came after our theoretical

superconductivity, and, finally, the unsolved problem in 3D.

2. Models

We consider a system of spin-$1/2$ fermions described by a general multi-band Hamiltonian of the form

$$\mathscr{H} = \mathscr{H}_K + \mathscr{H}_{\rm int}; \quad \mathscr{H}_K = \sum_{\mathbf{k},m,\sigma} \epsilon_m(\mathbf{k}) c^\dagger_{\mathbf{k}m\sigma} c^\dagger_{\mathbf{k}m\sigma}, \tag{1}$$

where $\mathbf{k}$ is crystal momentum, m is a band label, and σ the spin. $\mathscr{H}_K$ describes the kinetic energy of the "low-energy" bands that are impacted by superconductivity; we ignore bands far from the chemical potential that are either fully occupied or completely empty. The external vector potential $\mathbf{A}$ enters $\mathscr{H}$ through the Peierl's substitution in the tight-binding representation of $\mathscr{H}_K$ or minimal subtraction in a continuum model. We consider an arbitrary interaction term $\mathscr{H}_{\rm int}$ that leads to pairing and superconductivity, with the single assumption that $\mathbf{A}$ does *not couple* to $\mathscr{H}_{\rm int}$. These are very natural assumptions in most theoretical models of superconductivity, including the usual electron–phonon interaction, electron–electron interactions like in the Hubbard model, and super-exchange in the tJ model. The assumptions are also valid for the Feshbach resonance that leads to pairing of ultracold Fermi atoms, with rotation playing the role of the magnetic field.

We postpone until Sec. 10 the discussion of cases in which these assumptions are not valid, and the analysis then becomes more involved.[2] We discuss in that section T_c bounds for models of flat-band superconductivity, where $\mathscr{H}_K \equiv 0$, as well as topological bands, where the Wannier functions are not exponentially localized, and thus, tight-binding and Peierl's substitution cannot be used straightforwardly. For now, we focus on the class of Hamiltonians described in the preceding paragraph, which after all have very broad applicability.

3. Bounds on Superfluid Stiffness

amplitude of the order parameter or (2) by destroying phase coherence, even though the amplitude is robust. BCS-Eliashberg mean-field theory falls into the first category, with the transition temperature $T_c \propto |\Delta|$, the superconducting gap. The BKT theory of vortex–antivortex unbinding in 2D falls into the second category, as do the ideas of Uemura[8] and of Emery–Kivelson[10] in 3D. When phase fluctuations control the destruction of superconductivity $T_c \propto D_s$, the superfluid stiffness, and we will focus on bounding D_s.

The superfluid stiffness controls the free energy cost $\frac{D_s}{2}\int d^d\mathbf{r}|\nabla\theta|^2$ of distorting the phase of the SC order parameter $|\Delta|e^{i\theta}$ and is related to the London penetration depth in 3D via $1/\lambda_L^2 = (4\mu_0 e^2/\hbar^2)D_s$. The stiffness is essentially the same as the helicity modulus Υ of Michael Fisher and coworkers.[11]

Microscopically, D_s can be calculated using linear response theory[12,13] :

$$D_s = \widetilde{D} - \frac{\hbar^2}{4e^2}\chi^{\perp}_{j_x j_x}(\mathbf{q}\to 0, \omega = 0),$$

(2)

where $\widetilde{D}$ is the "diamagnetic term", of central interest in this work, and $\chi^{\perp}_{j_x j_x}$ is the transverse paramagnetic current–current correlation function. We use the Lehmann representation to obtain $\chi^{\perp}_{j_x j_x}(\mathbf{q}\to 0, \omega = 0) \geq 0$, as can be seen from

$$\chi^{\perp}_{j_x j_x} = \frac{1}{\mathscr{Z}}\sum_{ij}\left[\frac{e^{-\beta E_i} - e^{-\beta E_j}}{E_j - E_i}\right]|\langle i|j_x^P(\mathbf{q})|j\rangle|^2,$$

(3)

using $(e^{-x} - e^{-y})/(y - x) \geq 0$. Here, $|i\rangle$'s are the exact eigenstates of $\mathscr{H}$ of Eq. (1) with eigenvalues E_i and the partition function $\mathscr{Z} = \mathrm{Tr}[e^{-\beta\mathscr{H}}]$, with $\beta = 1/k_B T$. We thus obtain a rigorous upper bound

$$D_s(T) \leq \widetilde{D}(T).$$

(4)

back

II. Optical Spectral Weight

Before turning to the question how one can calculate $\widetilde{D}$, let us develop some intuition for what it means and why it gives an upper bound on the superfluid stiffness. Using the Kubo formula for the frequency-dependent conductivity $\sigma(\omega)$ and the Kramers–Krönig relation, it is straightforward to derive the optical sum rule

$$\int_0^\infty d\omega \mathrm{Re}\sigma(\omega) = \frac{2\pi e^2}{\hbar^2}\widetilde{D}, \tag{5}$$

where the frequency integration includes all the "low-energy" bands (but excludes the fully occupied or completely empty bands that were not part of Eq. (1)). By identifying $\widetilde{D}$ with the *optical spectral weight*, we see that it is gauge-invariant. Moreover, the second law of thermodynamics implies that the dissipative response $\mathrm{Re}\,\sigma(\omega) \geq 0$, and thus, so is $\widetilde{D}$.

Now, in any superconductor $\mathrm{Re}\,\sigma(\omega) = (4\pi e^2 \,/\, \hbar^2) D_s \delta(\omega) + \mathrm{Re}\,\sigma_{\mathrm{reg}}(\omega)$, where the singular term describes the infinite d.c. conductivity of the condensate and the "regular" term is a non-negative contribution arising from excitations. Using the sum rule (5), it is easy to understand the inequality of Eq. (4).

Next, we turn to computing the optical spectral weight for our model. From the linear response calculation that leads to Eq. (2), we see that $\widetilde{D}$ is essentially $\langle \partial^2 \mathscr{H} \,/\, \partial A_x^2 \rangle$, and thus, we find

$$\widetilde{D}(T) = \frac{\hbar^2}{4V} \sum_{\mathbf{k},mm',\sigma} M^{-1}_{mm'}(\mathbf{k}) \langle c^\dagger_{\mathbf{k}m\sigma} c^\dagger_{\mathbf{k}m'\sigma} \rangle. \tag{6}$$

For a simple parabolic band with dispersion $\epsilon(\mathbf{k}) = \hbar^2 k^2 \,/\, 2m$, the optical spectral weight $\widetilde{D} = \hbar^2 n \,/\, 4m$ is proportional to the plasma frequency. For non-parabolic dispersion or multiple bands, however, one cannot uniquely decompose $\widetilde{D}$ into the ratio of a density and a mass. In the

is replaced by the density matrix (V is the volume of the system).

The inverse mass matrix is given by

$$M^{-1}_{mm'}(\mathbf{k}) = \sum_{\alpha\beta} U^*_{m,\alpha}(\mathbf{k}) \frac{\partial^2 t_{\alpha\beta}(\mathbf{k})}{\partial(\hbar k_a)^2} \; U_{\beta,m'}(\mathbf{k}),$$

(7)

where α, β label orbitals/sites within a unit cell (labeled by i) of a Bravais lattice, $t_{\alpha\beta}(\mathbf{k})$ is the Fourier transform of the hopping matrix element $t_{\alpha\beta}(\mathbf{r}_{i\alpha} - \mathbf{r}_{j\alpha})$, and $U_{\alpha,m}(\mathbf{k})$ is the unitary transformation that diagonalizes $t_{\alpha\beta}(\mathbf{k})$ to obtain the band structure: $U^*_{m,\alpha}(\mathbf{k}) t_{\alpha\beta}(\mathbf{k}) U_{\beta,m}(\mathbf{k}) = \epsilon_m(\mathbf{k}) \delta_{m,m'}$. Note that M^{-1} depends only on band dispersion and Bloch wave functions, and not on interactions or temperature. The density matrix $\langle c^\dagger_{\mathbf{k}m\sigma} c_{\mathbf{k}m'\sigma} \rangle$ in Eq. (6), on the other hand, depends in general on both interactions and temperature, since the equilibrium expectation value is computed using $\exp(-\mathscr{H} \,/\, k_B T) \,/\, \mathscr{Z}$.

5. T_c Bounds in Two Dimensions

The optical spectral weight bound on the superfluid stiffness is valid in any dimension. Now, we restrict attention to *two dimensions* (until Sec. 11), since it is only in 2D that there is a universal relation between the BKT transition temperature and the superfluid stiffness. $D_s(T)$ exhibits a jump discontinuity at T_c and the RG analysis[14] of Nelson and Kosterlitz leads to the celebrated result $k_B T_c = \pi D_s(T_c^-) \,/\, 2$. Remarkably, the 'amplitude ratio' $\pi \,/\, 2$ is universal; it is related to value of the critical exponent $\eta(T_c^-) = 1 \,/\, 4$.

Combining this result with Eq. (4), we obtain a bound on T_c, namely

$$k_B T_c \leq \frac{\pi}{2} \widetilde{D}(T_c),$$

(8)

strength, but is it useful? In the rest of this paper, I show that there are many situations where this bound leads to insights into the T_c of strongly correlated superconductors with low-density and narrow bands, systems where the standard BCS-Eliashberg mean-field approach fails. Conversely, in regimes where mean-field theory works, the bound is still valid but not useful, since it gives a huge overestimate.

6. Parabolic Bands and 2D BCS–BEC Crossover

Consider the problem of superconductivity in a 2D parabolic band with dispersion $\hbar^2k^2 \,/\, 2m$, density n, or Fermi energy $E_F = \pi\hbar^2 \,/\, n \,/\, m$, and arbitrary interaction that leads to pairing. We can then write the stiffness $D_s(T) = \hbar^2 n_s(T) \,/\, 4m$ in terms of the *superfluid density* $n_s(T)$, and our bound of Eq. (4) reduces to the simple statement that the superfluid density $n_s(T) \leq n$ is the total density. Equation (8) then leads to the inequality

$$k_B T_c \leq \frac{1}{8} E_F. \tag{9}$$

Plotting the line $k_B T_c = E_F \,/\, 8$ on the Uemura plot looks very nice and gives a general scale for the limits on T_c, as seen in Fig. 1. But we should caution that only few of the systems on that plot fulfill the condition of parabolic bands in 2D. In that sense, this is like a “Drude model” result that gives a sense of what should happen, but if one looks at multi-band systems with complicated band structures, only the optical spectral weight bound is justified.

This raises the question: Can one experimentally test this bound for parabolic bands? This can definitely be tested in the BCS–BEC crossover in 2D (which we discuss in the following) in experiments and in quantum Monte Carlo simulations of the ultracold Fermi gases. But, surprisingly, the first experimental test has been in a quantum material. To investigate the BCS–BEC crossover, one needs to tune $\Delta \,/\, E_F$, the ratio of the gap to Fermi energy. Unlike cold atoms, where the Feshbach resonance is used to control Δ, there is no way in general to tune the

intercalation and ionic liquid gating, the Iwasa group was able to change the density, and thus the Fermi energy, by *two orders of magnitude* and investigate the BCS–BEC crossover in $\mathrm{Li}_x\mathrm{ZrNCl}$.[4] Electronic structure calculations[15] show that this 2D material has a parabolic band.

The experiments measure the electron density using the Hall effect and probe superconducting properties, like the pair size ξ_0 (from the upper critical field) and energy gap Δ (from tunneling). As the density is decreased by gating, the measured values of $1 / (k_F \xi_0)$ and Δ / E_F show clear evidence of tuning into the strongly interacting BCS–BEC crossover regime, as well as the characteristic normal state pairing pseudogap seen in tunneling.

Remarkably, the measured values of $k_B T_c / E_F$ increase upon approaching the crossover regime and then saturate at a value of 0.12, very close to the predicted 1/8, as can be seen in Fig. 1.

We next discuss in more detail the BCS–BEC crossover in 2D dilute Fermi gases; see Fig. 2. These systems are dilute in the sense that the range of the interaction is much smaller than $1 / k_F$. The 2D crossover for s-wave pairing is parametrized by the dimensionless interaction $\log(E_b / E_F)$, where E_b is the binding energy of the two-body bound state in vacuum.[16] In the weak-coupling BCS limit $E_b / E_F \ll 1$, the pair size $\xi_0 \gg 1 / k_F$. The mean field T_c has a BCS essential singularity and is exponentially smaller than our bound. In the opposite BEC limit $E_b / E_F \gg 1$, the bosons of size $\xi_0 \ll 1 / k_F$ have mass $2m$, density $n / 2$ and an inter-boson scattering length a_b, which has been computed[17] in terms of E_b. Here too, our bound is larger than $k_B T_c \sim E_F / \log\log(\text{const.}\, E_b / E_F)$,[18,19] valid in the regime $\log\log \gg 1$. Thus, $T_c \to 0$ in the extreme BEC limit, as it must for non-interacting bosons, but does so extremely slowly. These results are shown in a schematic phase diagram in Fig. 1, where we see that $E_F / 8$ is likely to be saturated in the crossover regime with pair size ξ_0 or order the interparticle spacing $1 / k_F$.

back

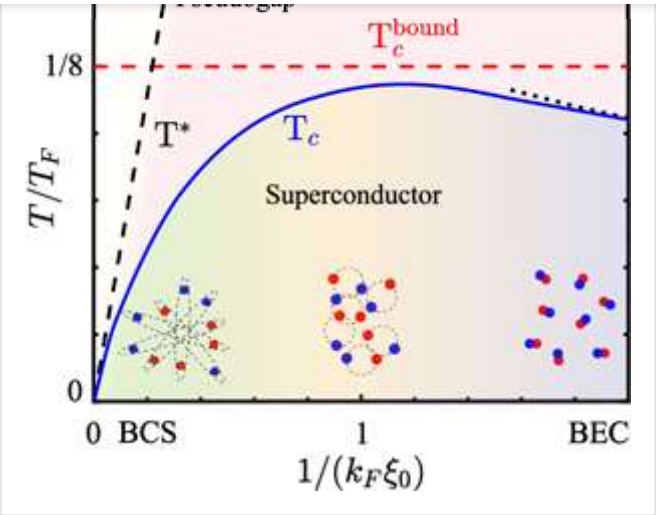

Fig. 2. (Color online) Schematic phase diagram of the BCS–BEC crossover in a 2D Fermi gas with short-range attractive interactions. The ratio of the inter-particle separation $1 / k_F$ to the pair size ξ_0 shows how the attraction between fermions increases from the BCS regime of large pairs to the BEC of tightly bound pairs. The blue curve is the schematic transition temperature T_c (in units of the Fermi temperature $T_F = E_F / k_B$), which interpolates between known results in the BCS and BEC limits; see text. T_c vanishes in the extreme BEC limit in 2D, but does so very slowly (double logarithm), as indicated by the dotted asymptote; see text. The black dashed line is the pseudogap temperature T^* below which pairs form, while superconductivity develops only below the BKT T_c. The red dashed line is the theoretical limit $Tc \leq T_F / 8$ for parabolic dispersion.

To conclude this section, we note that a transition temperature of $E_F / 8$ was seen in various approximate calculations (using mean-field theory plus fluctuations) for 2D models for cold atoms[20,21] and for quantum materials[22], with parabolic band structures and specific choices of pairing interactions. But the generality of the result as an upper bound independent of the nature of the interactions was not recognized. In fact, some of these approximate calculations[20] obtained the erroneous result that $E_F / 8$ was the T_c in the extreme BEC limit, where, in fact the T_c is known to vanish, as discussed above.

7. Non-Parabolic Dispersion

For a single band with arbitrary dispersion $\epsilon(\mathbf{k})$, Eq. (6) simplifies to

$$\widetilde{D} = \frac{1}{4V}\sum_{\mathbf{k}\sigma}\frac{\partial^2\epsilon}{\partial k_x^2}n(\mathbf{k}),$$

(10)

where $n(\mathbf{k}) = \langle c^\dagger_{\mathbf{k}\sigma} c_{\mathbf{k}\sigma}\rangle$ is the momentum distribution. For the specific case of nearest neighbor hopping on a square lattice $\epsilon(\mathbf{k}) = -2t[\cos(k_x a) + \cos(k_y a)]$ and $\widetilde{D}$ is proportional to the thermal expectation value of the kinetic energy $\langle \mathrm{KE}\rangle$. The optical spectral weight in lattice systems is often just called "kinetic energy." This identification is true neither for a single band with arbitrary dispersion nor for a multi-band system. (In the latter case, Eq. (6) depends not only on the dispersion but also on the single-particle wave functions through the U-matrix.)

It is instructive to compare our bound for the single band $\widetilde{D}$ with sign-problem-free Quantum Monte Carlo (QMC) simulations[23] of the attractive Hubbard model on a 2D square lattice, with $\mathscr{H}_{\mathrm{int}} = -|U|\sum_i (n_{i\uparrow} - 1/2)(n_{i\downarrow} - 1/2)$. For a density $n \neq 1$, the system has a superconducting ground state, exhibiting a crossover from a weak coupling BCS state ($|U|/t \ll 1$) to a BEC of hard-core on-site bosons ($|U|/t \gg 1$). The QMC result[23] for T_c is a non-monotonic function of $|U|/t$ at a fixed density n. The BCS mean-field theory correctly describes the weak coupling $T_c \sim t\exp(-t/|U|)$, but for $|U|/t \gtrsim 2$, the mean field "T_c" represents a pseudogap[24,25] crossover temperature T^* below which pairs form and which lies well above the QMC T_c, at which phase coherence is established. The two scales exhibit quantitatively different behaviors at large $|U|/t$, where $T^* \sim |U|$, while $T_c \sim t^2/|U|$ the effective boson hopping.

Using the triangle inequality and $n(\mathbf{k}) \leq 1$, it is easy to see that we get $k_B T_c \leq \pi\widetilde{D}/2 \leq (\pi/4V)\sum_{\mathbf{k},\boldsymbol{\sigma}} |\partial^2\epsilon/\partial k_x^2|$. This U-independent bound is obviously better than the MFT "T_c" that diverges as $|U|$ at strong coupling. The use of $n(\mathbf{k}) \leq 1$ is too crude, however, to capture the $t^2/|U|$ asymptotic behavior of T_c. We can use $n(\mathbf{k})$ as obtained from the Leggett crossover theory of the BCS–BEC crossover[9] in Eq. (10) to get an *estimate* (rather an exact bound) on T_c. This leads to an "approximate bound" that goes to a constant at small $|U|$ and crosses over to $t^2/|U|$ behavior at large $|U|$. In summary, we see that at weak coupling, the $\widetilde{D}$

Hubbard model. The reader is referred to Fig. 2 and related discussion in Ref. **1** for details.

8. Multi-Band Systems

In the general multi-band case, we need to deal with the density matrix of the interacting system about which we have little *a priori* knowledge. We can, however, proceed as follows. $\widetilde{D} \geq 0$ from the optical sum rule, and we use the triangle inequality to obtain $\widetilde{D} \leq \frac{\hbar^2}{4V} \sum_{\mathbf{k},mm',\sigma} |M^{-1}_{mm'}(\mathbf{k})||\langle c^\dagger_{\mathbf{k}m\sigma} c_{\mathbf{k}m'\sigma}\rangle|$. Next, we define an inner product in the space of operators $(A, B) = \langle A^\dagger B\rangle$ in terms of a thermal expectation value. This allows us to use the Cauchy–Schwarz inequality $|\langle c^\dagger_{\mathbf{k}m\sigma} c_{\mathbf{k}m'\sigma}\rangle| \leq [n_m(\mathbf{k})\, n_{m'}(\mathbf{k})]^{1/2}$, where $n_m(\mathbf{k}) = \langle c^\dagger_{\mathbf{k}m\sigma} c_{\mathbf{k}m\sigma}\rangle$ is the momentum distribution of the m^{th} band. Now, for any Fermi system, $n_m(\mathbf{k}) \leq 1$, and we obtain by this sequence of inequalities that $\widetilde{D} \leq \frac{\hbar^2}{4V} \sum_{\mathbf{k},mm',\sigma} |M^{-1}_{mm'}(\mathbf{k})|$.

In fact, a better bound is obtained by first transforming the sum on right-hand side of Eq. (6) to a basis in which $M^{-1}_{mm'}(\mathbf{k})$ is diagonalized and then using this sequence of inequalities, we then obtain

$$k_B T_c \leq \frac{\pi}{2} \widetilde{D}(T_c) \leq \frac{\pi}{2} \frac{\hbar^2}{4V} \sum_{\mathbf{k},a,\sigma} |\lambda_a(\mathbf{k})|, \tag{11}$$

where $\lambda_a(\mathbf{k})$'s are the eigenvalues of $M^{-1}_{mm'}(\mathbf{k})$. We have greatly degraded the bound, so the final result is likely to be a large overestimate, nevertheless, we have arrived at a general multi-band bound that depends only on the band structure and is independent of the mechanism of superconductivity.

9. 2D Materials

In this section, we apply our bound to various strongly correlated 2D superconductors. We have already discussed the gate-controlled BCS–BEC crossover in Li:ZrNCl[4] in Sec. 6. Here, we briefly discuss Monolayer FeSe/STO and magic angle twisted bilayer graphene.

K, with some reports of T_c as high as 109 K; for a review, see Ref. **6**. This is remarkable since bulk FeSe has a T_c around 10 K and free-standing monolayers are not superconducting even at temperatures as low as 2 K. There is no consensus on the pairing mechanism and the role of the substrate in increasing T_c. Our bound is useful here because it is agnostic to the pairing mechanism, symmetry of the order parameter, and other issues under debate.

We use an effective two-orbital model consistent with $\mathbf{k}\cdot\mathbf{p}$ perturbation theory that describes the two electron pockets around the M-point of the Brillouin zone,[27,28] and fit the parameters of the electronic structure to ARPES data.[29] The orbitals derive from the same two-dimensional irreducible representation and the Fermi surfaces are small so we can truncate the $\mathbf{k}\cdot\mathbf{p}$ dispersion at quadratic order in k_x and k_y. We thus find that the inverse mass $M^{-1}_{mm'}(\mathbf{k})$ turns out to be proportional to $\delta_{m,m'}$ and $\mathbf{k}$-independent. Thus, the $\mathbf{k}$-sum in Eq. (6) is simply proportional to the Fermi energy, and we find $T_c \leq 164$ K; see Ref. **26**.

Magic angle twisted bilayer graphene (MA-TBG): There has been an explosion of interest in MA-TBG, where superconductivity was first reported[5] in the vicinity of correlation-induced insulating state. This is not the place to review the large, and ever-growing, experimental and theoretical literature on this topic; however, it is safe to say that there is at present no consensus on the pairing mechanism (phonons versus correlations) or the symmetry of superconducting order parameter.

The electronic band structure of MA-TBG is complex. There are 8 ($= 4 \times 2$ for spin degeneracy) narrow bands,[30] with a total bandwidth $\lesssim 10$ meV, and these bands have non-trivial topology.[31,32] There is much discussion in the literature about whether inclusion of additional bands may help deal with both the topology and the interactions. There is also the issue of whether one can write down a tight-binding model for the low-energy bands and have an effective interaction such that the vector potential couples only to the kinetic energy. We address these questions in Sec. 10, where we obtain T_c bounds for simple models of flat-band superconductivity.

For now, we simply focus on models of MA-TBG that meet the conditions spelled out at the outset in Sec. 2. We use the tight-binding model of Ref. **33**, which is a multi-parameter fit to the

tight-binding models[34] for MA-TBG. We compute the inverse mass matrix $M^{-1}_{mm'}(\mathbf{k})$ from the tight-binding model and then use Eq. (11) to find that $T_c \leq 48\,\mathrm{K}$. This is a large overestimate because we have degraded the inequality in Sec. 8 as explained above.

10. Flat-Band Superconductors

In recent years, there has been interest in the effect of correlations in flat bands that has only intensified following the discovery of superconductivity in magic-angle-twisted bilayer graphene (MA-TBG). There has been important progress on the *mean-field theory* (MFT) of flat-band superconductivity[35,36,37,38,39] in attractive (negative U) Hubbard models. The gap scale was found to be proportional to $|U|$ and the superfluid stiffness proportional to $|U|$ times the trace of the quantum metric $\sum_{\mathbf{k}} \mathrm{Tr} g(\mathbf{k})$ for the flat-band wave functions. The *quantum metric* $g_{ab}(\mathbf{k})$ defined by $ds^2 = 1 - |\langle \psi(\mathbf{k}+d\mathbf{k})|\psi(\mathbf{k})\rangle|^2 = g_{ab}(\mathbf{k}) dk_a dk_b$ characterizes the distance between states in Hilbert space.[40,41]

But to what extent should one trust MFT in a problem where the attractive interaction $|U|$ is much larger in the bandwidth, in fact, infinitely larger in the flat-band limit? Our goal was to find an exact bound on D_s, for which we need to face up to multiple challenges. First, if we use the multi-band bound derived above, we find that it is far from optimal, since it includes optical spectral weight from inter-band transitions, while we would like to focus only on intra-band spectral weight to get a tight bound. Second, if one projects down to the flat band to focus on the intra-band spectral weight, there is no kinetic energy term, and thus one cannot couple the vector potential $\mathbf{A}$ to flat-band KE as we had done above. Finally, there is a lot of interest in topological flat bands, motivated by MA-TBG. Non-trivial band topology, however, acts as an obstruction to finding exponentially localized Wannier functions obeying all the symmetries of the problem, and one cannot write down a tight-binding Hamiltonian describing the topological bands alone.

All of these challenges have been addressed for both non-topological and topological flat bands with an attractive Hubbard interaction in Ref. **2**. Omitting all technical details of the derivations, we summarize the main results. Note that flat bands cannot exist “in isolation” and arise in models, such as the Lieb lattice, with multiple orbitals in each unit cell. We work in a regime

$w \ll |U| \ll E_0$, the gap between the flat band and other bands. We project onto the flat band and focus on the low-energy (intra-band) optical spectral weight $\widetilde{D}_{\rm low} = (\hbar^2 \,/\, 2\pi e^2) \int_0^\Lambda d\omega \, {\rm Re}\sigma(\omega)$, where the upper cutoff satisfies $|U| \ll \Lambda \lesssim E_0$.

For the Lieb lattice, one finds an exactly flat band at zero energy and two p–h symmetric dispersive bands, using "staggered hopping" to open up the gap E_0. We can then derive an upper bound $\widetilde{D}_{\rm low} \leq \widetilde{n}|U|\Omega \,/\, 2$. Quite naturally, $|U|$ sets the scale of the optical weight, since there is no transport in a flat band in the absence of interactions. The dependence on the density *n* comes in via $\widetilde{n} = \min(n, 2-n)$, which vanishes, as expected for a completely empty/full flat band. Finally, Ω is the Marzari–Vanderbilt[41] spread of the flat-band Wannier function (WF). The optimal bound on $\widetilde{D}_{\rm low}$ is thus obtained by choosing the most highly localized WFs. The quantum metric prevents us from reducing this as much as we please, since $\Omega \geq \sum_{\mathbf{k}} {\rm Tr} g(\mathbf{k})$. The Lieb lattice has non-topological flat bands, and thus, the system can be continuously deformed into a trivial insulator where individual unit cells (each with three sites) become decoupled from each other. In this limit, $\Omega \to 0$ so that the optical spectral weight vanishes and that there is no transport.

Using $D_s \leq \widetilde{D}_{\rm low}$ and the BKT relation between T_c and D_s, we obtain $k_B T_c \leq \pi \widetilde{n}|U| \min \Omega \,/\, 4$. We note that for the Lieb lattice with its particle–hole symmetric band structure, it is natural to say that in the flat-band regime, $E_F = 0$. This re-emphasizes the point that there is in general no upper bound on $T_c \,/\, E_F$ and the only general bound on T_c is in terms of the optical spectral weight.

Many authors have emphasized lower bounds on D_s arising from a mean-field approximation.[36,37,38,39] Using the well-known inequality,[41] ${\rm Tr} g(\mathbf{k}) \geq \mathscr{C}$, it is easy to see that the mean field D_s, proportional to the trace of the quantum metric, is bounded below by the Chern number $\mathscr{C}$, We emphasize that these mean-field 'bounds' are not exact lower bounds, since fluctuations ignored in mean-field theory would be expected to reduce the superfluid stiffness.

We can also obtain an *exact lower bound* on $\widetilde{D}_{\rm low}$ at $T = 0$ by exploiting rigorous mathematical physics results[43] on the off-diagonal long-range order (LRO) in the ground state of the attractive Hubbard model on the Lieb lattice. (This result is the $U < 0$ counterpart of Lieb's theorem on

$\widetilde{D}_{\rm low} \geq \widetilde{n} \sum_{\mathbf{k}} {\rm Tr} g(\mathbf{k}) \,/\, 72.$

Finally, we briefly summarize our bounds on D_s in *topological* flat bands. The tight-binding model of Ref. **44** has flat bands with $\mathbb{Z}_2$ odd topology, and one cannot obtain localized WFs with a finite spread Ω. There are two degenerate, (nearly) flat bands $|\mathbf{k}\uparrow\rangle$ and $|\mathbf{k}\downarrow\rangle$ with spin Chern numbers $\mathscr{C}_{\uparrow,\downarrow} = \pm 1$. Using the methodology developed in Refs. **45** and **46**, we "unwind the topology" and find two linear combinations $|\mathbf{k}\,1\rangle$ and $|\mathbf{k}\,2\rangle$, both of which have zero Chern number. The price we pay is that the corresponding exponentially localized WFs are not a Kramers pair and the states have a non-local representation of time-reversal symmetry. Nevertheless, this allows us to proceed with our analysis, and the resulting upper bound on $\widetilde{D}_{\rm low}$ is proportional to $|U|$, to $\widetilde{n} = \min(n, 2-n)$, and to a generalized second moment of the WFs. The bound is also found to compare favorably with D_s computed using sign-problem-free QMC simulations[47] for the same model; see Ref. **2** for details.

11. T_c in Three Dimensions

Given the success in bounding T_c in 2D, it is natural to ask: What about 3D? Experiments seem to suggest at first sight that there might well be such a bound on T_c in 3D systems; see the Uemura plot in Fig. 1. For example, the BCS–BEC crossover in 3D experiments and quantum Monte Carlo calculations suggest that $\max T_c \simeq 0.22 E_F \,/\, k_B$; see Ref. **9** for a more detailed discussion and references. But there are no rigorous bounds available on T_c in 3D even though the optical spectral weight bound on the superfluid stiffness of Eq. (4) is valid in *any* dimension. We now discuss the challenges for deriving such bounds and whether they even exist.

First, there is a widespread misconception that the non-interacting BEC temperature $k_B T_{\rm BEC} = [n \,/\, 2\zeta(3\,/\,2)]^{2/3} \pi\hbar^2 \,/\, m \simeq 0.218 E_f$ of tightly bound pairs (bosons with density $n\,/\,2$ and parabolic dispersion with mass $2m$) provides an "upper bound" to the transition temperature of a strongly coupled superconductor. However, it is now rigorously established in the mathematical physics literature that the T_c of the dilute Bose gas in 3D is *higher* than the non-interacting BEC temperature. The reader is directed to Ref. **48** for the proof, as well as a summary of the decades-long history of incorrect statements on this issue by a long list of luminaries!

cost for phase distortions $\mathscr{F} = \frac{\nu_s}{2} \int d^d\mathbf{r} |\nabla\theta|^2$, we see that D_s has dimensions of energy *only* in 2D, and this underlies the universal relation between T_c and D_s in the BKT theory. If thermal phase fluctuations govern the 3D transition, then following Ref. **10**, $k_B T_c = \mathscr{C} D_s(0) \bar{a}$, where $\bar{a}$ is a "cutoff" length scale, the scale up to which one has to coarse-grain the underlying fermionic model to derive an effective XY model, and $\mathscr{C}$ is a *non-universal* constant. Given a cutoff $\bar{a}$, one would need to bound $\mathscr{C}$ to get a bound on T_c. See Ref. **1** for further discussion.

From a practical point of view, one is interested in learning how high T_c can be in a class of models or materials. But, if a general bound were to exist, it should be equally valid in situations where both T_c and D_s are driven to zero near a quantum critical point (QCP). Quantum Josephson scaling[49] implies $D_s(0) \sim \delta^{(z+d-2)\nu}$ in the vicinity of a QCP tuned by the dimensionless parameter $\delta \to 0^+$, where ν is the correlation length exponent and z the dynamical exponent in d spatial dimensions. Using $T_c \sim \delta^{z\nu}$, one obtains $T_c \sim D_s^{z/(z+d-2)}$. Thus, in 2D, one finds $T_c \sim D_s$, independent of z. However, in 3D, one obtains $T_c \sim D_s^{z/(z+1)}$, a sub-linear scaling sufficiently close to the QCP which necessarily violates any proposed upper bound on T_c that scales linearly with D_s. Such a sub-linear scaling is indeed observed in experiments in highly underdoped[50,51] and highly overdoped[52,53] cuprates, with $T_c \sim D_s^{1/2}$ consistent with $z = 1$. Thus, the linear scaling between T_c and D_s, central to the 2D bounds presented above, is necessarily violated near a 3D QCP.

12. Conclusions

In conclusion, I take this opportunity to record my gratitude to Michael Fisher for taking me under his wing when I first moved to Cornell as a graduate student, even though his sabbatical plans led me to eventually do my thesis research under Jim Sethna's supervision. I am grateful for much that I learned from Michael while working on the two papers[54,55] that I wrote with him (and one that we never finished) and for his amazing lectures on critical phenomena and RG, whose notes I still refer back to after so many years.

Acknowledgments

Ph.D. thesis of Tamaghna Hazra (now at Rutgers) and of Nishchhal Verma (now at Columbia), whose contributions are gratefully acknowledged. I acknowledge the support from the NSF Materials Research Science and Engineering Center Grant DMR-2011876.

ORCID

Mohit Randeria https://orcid.org/0000-0001-8566-5930

Note

[a] 'Rigorous' is used here in the sense of theoretical physics, i.e. an exact result; however, we do not address subtleties of the thermodynamics limit that mathematical physicists would care about.